PCCP

Accepted Manuscript

ROYAL SOCIETY OF CHEMISTRY

www.rsc.org/pccp

Graphic abstract

Excitation of hematite with visible light promotes electron transfer from the dissimilatory metal-reducing species *Geobacter sulfurreducens* to hematite surface.

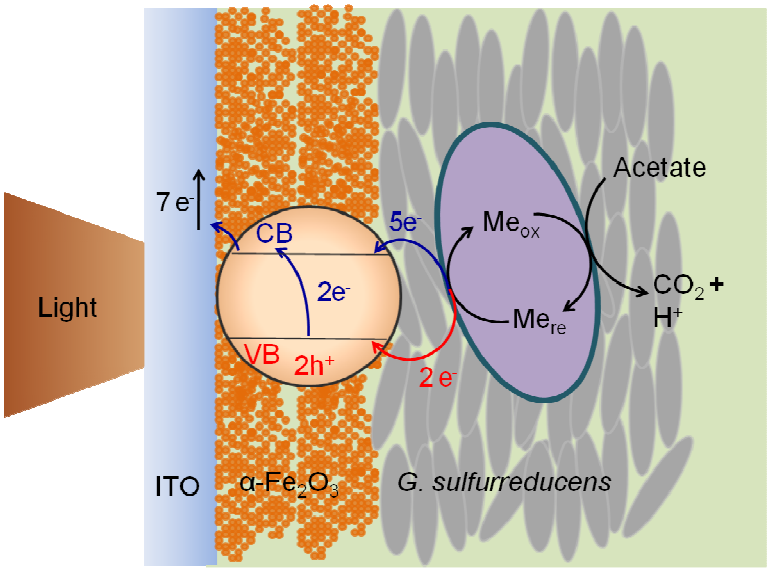

Light-driven microbial dissimilatory electron transfer to hematite†

Dao-Bo Li, Yuan-Yuan Cheng, Ling-Li Li, Wen-Wei Li, Yu-Xi Huang, Dan-Ni Pei, Zhong-Hua Tong, Yang Mu, Han-Qing Yu*

Department of Chemistry, University of Science & Technology of China, Hefei, 230026, China

Corresponding author: Fax: +86-551-63607592, E-mail: hqyu@ustc.edu.cn

† Electronic supplementary information is available.

Abstract

The ability of dissimilatory metal-reducing microorganisms (DMRM) to conduct extracellular electron transfer with conductive cellular components grants them a great potential for bioenergy and environmental applications. Crystalline Fe(III) oxides, a type of widespread electron acceptor for DMRM in nature, can be excited by light for photocatalysis and microbial culture-mediated photocurrent production. However, the feasibility of direct electron transfer from living cells to light-excited Fe(III) oxides has not been well documented and the cellular physiology in this process has not been clarified. To resolve these problems, an electrochemical system composed with *Geobacter sulfurreducens* and hematite (α-Fe_2O_3) was constructed, and direct electron transfer from *G. sulfurreducens* cells to the light-excited α-Fe_2O_3 in the absence of soluble electron shuttles was observed. Further studies evidenced the efficient excitation of α-Fe_2O_3 and the dependence of photocurrent production on the biocatalytic activity. Light-induced electron transfer on the cell-α-Fe_2O_3 interface correlated linearly with the rates of microbial respiration and substrate consumption. In addition, the *G. sulfurreducens* cells were found to survive on the light-excited α-Fe_2O_3. These results prove a direct mechanism behind the DMRM respiration driven by photo-induced charge separation in semiconductive acceptors and also imply new opportunities to design photo-bioelectronic devices with living cells as a catalyst.

Broader context

This study reports a light-driven electron transfer from dissimilatory metal-reducing microorganisms (DMRM) to crystalline Fe(III) oxides. Both photochemistry and the dissimilatory metal reduction phenomenon have been recognized for many years, but the connection between the light-excited charges on semiconductors and the energy metabolism of DMRM species has received little attention. In this work, we demonstrate that light illumination substantially accelerated the electron transfer from *Geobacter sulfurreducens* to α-Fe_2O_3. The microbial cells on the α-Fe_2O_3 surface are not damaged by the photo-generated holes. Such a light-driven electron transfer from DMRM cells to Fe(III) oxides suggests a unique way of energy communication between the organic lives and the inorganic minerals in nature. These findings broaden our understanding about the microbial respiration and potential bioenergy applications.

Introduction

Exploiting the capability of microorganisms in extracellular electron transfer has drawn great interests in recent years for bioenergy and environmental remediation applications[1-3]. Many dissimilatory metal-reducing microorganisms (DMRM) are able to utilize extracellular solid-state electron acceptors such as carbon materials and metal oxides[4], in which processes extracellular electron transfer plays a central role[5]. A set of sophisticated complexes consisting of conductive pili and associated c-type cytochromes (cyt. c) is found to stretch from the cellular membrane of DMRM directly to the solid surface, breaking the physical barrier caused by insulating phospholipid bilayer[6].

Crystalline Fe(III) oxides are one of the most common natural electron acceptors for DMRB[7,8]. Electron transfer from microbial cells to these oxides is of fundamental importance for several processes. Fe(III) oxide-based bioanode significantly improved the electricity generation in bioelectrochemical systems, probably because of the specific affinity between the oxide surface and cyt. c on the cell membrane as well as the increased contact area[9,10]. Besides, biogeochemical reduction of Fe(III) to Fe(II) in subsurface and aquatic sediments can be driven by the respiration of DMRM, accompanied with oxidative degradation of organic contaminants such as aromatic compounds[8].

Crystalline Fe(III) oxides can be excited by light irradiation, generating electron-hole pairs in the lattices. The light-excited electron-hole pairs improve both internal conductivity for enlarged charge density and oxidation kinetics on the surface for hole accumulation[11,12], which is beneficial for interfacial electron transfer. Thus, a gated electron transfer process from microbial enzymes to crystalline Fe(III) oxides might be possible in the presence of light. Similarly, photocurrent production catalyzed by microbial cultures (*Shewanella* spp.)[10,13,14] or peroxidase[15] on hematite has been demonstrated to be feasible for exploiting energy devices. However, since electron transfer from *Shewanella* spp. to acceptors is mainly mediated by flavins[16,17], the role of *Shewanella* cells in the photocurrent production and the cellular physiology on α-Fe_2O_3 surface are not clear yet[13,14]. Direct electron transfer from microbial cells to light-excited semiconductors is an important scientific issue in the fields of microbiology and bioenergy, and is also a challenge because of the potential cytotoxicity caused by the light-generated charges[18,19]. Furthermore, microbial metabolism on such a high-energy surface of the light-excited semiconductor in the photocurrent production is another issue that has not been explored by now.

In this work, an environmentally ubiquitous DMRM strain, *G. sulfurreducens*, was interfaced on α-Fe_2O_3 surface to construct an electrochemical system to explore the above problems. *Geobacter sulfurreducens* was chosen because of its characteristics of direct electron transfer for respiration without the involvement of mediators, excellent surface adhesion and cell aggregation[20], and a much higher

efficiency for electron recovery in substrate oxidation, compared with other DMRM[21]. α-Fe_2O_3 is one of the main natural Fe(III) oxides widespread in the environment[7,22] and also commonly used in electrochemical devices for photocatalysis[11,18]. In our electrochemical system, α-Fe_2O_3 was deposited on optically transparent tin-doped In_2O_3 (ITO) (Fig. 1a) as the electrode for electron collection and electrochemical characterizations. *G. sulfurreducens* cells grew on the α-Fe_2O_3 surface and were verified to be electrochemically active. With this system, we aim to explore: 1) whether the light-generated holes on α-Fe_2O_3 surface could drive direct electron transfer from *G. sulfurreducens* cells to α-Fe_2O_3; 2) how the light-excitation of α-Fe_2O_3 would correlate with the microbial respiration and metabolism; and 3) what conditions were required to achieve such a charge transfer between α-Fe_2O_3 and *G. sulfurreducens* cells.

Results

Direct electron transfer from *G. sulfurreducens* cells to α-Fe_2O_3 in dark

G. sulfurreducens is able to use solid electrode as the electron acceptor for respiration[21]. At a potential of +0.2 V vs. SHE, active *G. sulfurreducens* cells colonized and proliferated on the α-Fe_2O_3 or ITO electrode surface, forming a layer of compact cell matrix (i.e., biofilm) with a thickness of approximately 30 μm (Fig. 1b and d, Supplementary Fig. S1). The α-Fe_2O_3 layer was prepared by electrophoretic

deposition of α-Fe_2O_3 nanoparticles (~30 nm) onto the ITO surface. This α-Fe_2O_3 layer, with an average thickness of 2.1 μm, formed sandwich structure with cells and the ITO electrode (Fig. 1c). The α-Fe_2O_3 nanoparticles were used here in order to improve the charge separation efficiency[12]. Light was applied on the ITO side to directly illuminate the α-Fe_2O_3 layer, while minimize light absorption by *G. sulfurreducens* cells and the electrolyte. In order to mimic the natural conditions, fully visible light irradiation was adopted. In the microbial respiration, electrons from acetate metabolism were transferred to the α-Fe_2O_3 surface (Fig. 1b), driven by the redox gradient across the biofilm[23]. The electrons were then further delivered to the ITO electrode through α-Fe_2O_3, instead of reductively dissolved α-Fe_2O_3, to form Fe^{3+}/Fe^{2+} couple in the electrochemical system (Supplementary Fig. S2). Thus, an interface for direct electron transfer from the cells to α-Fe_2O_3 was successfully constructed and maintained during the tests.

The global respiration rate of *G. sulfurreducens* cells on the α-Fe_2O_3 or ITO surface was monitored in terms of the generated current. The cells without direct contacting with the α-Fe_2O_3 or ITO surface could also pump electrons to these electrodes through an extracellular conductive network[24]. Accompanied with the biofilm development, the current initially exhibited an exponential increase and eventually leveled off on both the α-Fe_2O_3 and ITO (Fig. 1b). *G. sulfurreducens* cells on the α-Fe_2O_3 surface produced 6 times higher current than that on the ITO surface (230.2 μA cm^{-2} vs. 38.1 μA cm^{-2}), possibly owing to a larger specific surface area and

higher affinity of the α-Fe_2O_3 layer to the cells. The steady-state current contributed by the cells (scanning at 1 mV/s) was dependent on the polarization potential (Fig. 1e, 1 mV/s). The onset potential for cellular respiration was at -0.299 V, and the maximum microbial respiration rate was achieved at -0.043 V, both are consistent with previous reports[25]. Reversible oxidation and reduction peaks were observed in a fast scanning (100 mV/s), and the peak potentials coincided with the maximum respiration rate and the onset point respectively. These observations provide clear evidence for a direct electron transfer from *G. sulfurreducens* cells to the electrode by extracellular cyt. c[26,27]. The potential of the cell/α-Fe_2O_3 system declined rapidly to below -0.25 V upon circuit interruption. The amperometric i-t tests showed a potential gradient across the α-Fe_2O_3 layer, which provided driving force for electron transport through the α-Fe_2O_3 (Fig. 1f and Supplementary Fig. S3).

Photocurrent produced by the excitation of the cell-α-Fe_2O_3 system

Electron transport through α-Fe_2O_3 in the dark is thought to occur in the conduction band composed of Fe(3d) orbitals, while the charges in the valence band (O(2p) orbitals) are not free-flowing unless excited by light or heat[28]. Visible light with a wavelength below 564.7 nm can excite electrons into the conduction band and leave positive charges (holes) in the valence band. The holes diffuse to the cell-α-Fe_2O_3 interface and cause a sharp current promotion (photocurrent) (Fig. 2a), switching on the light-excited electron transfer at the cell-α-Fe_2O_3 interface.

Reproducible response to each illumination with an average photocurrent density of 50.0 μA cm^{-2} was observed, implying a role of the excited α-Fe_2O_3 in the electron transfer at the cell-α-Fe_2O_3 interface.

A certain potential difference across α-Fe_2O_3 is required to retard the recombination and produce free-flowing charges. The effect of electrode potential on the photocurrent production was examined in the cell/α-Fe_2O_3 system to verify the light-excitation of α-Fe_2O_3 and its interplay with the interfacial electron transfer (Fig. 2b). The current at low potentials (*Regions I*) under illumination exhibited a similar pattern to that in the dark and was light-insensitive. The photocurrent at the cell-α-Fe_2O_3 interface appeared at around -0.25 V and increased gradually as the potential increased until +0.071 V (*Region II*). At potentials higher than +0.071 V (*Region III*), the photocurrent production was limited by the rate of biocatalytic reactions, as was shown at high potentials in CV (Fig. 1e). The photocurrent eventually leveled off at 74.54 μA cm^{-2} and exhibited a 40.6% increase in electron conduction efficiency compared to that in the dark. Promotion of conductivity in the cell-α-Fe_2O_3 system was also evidenced by the photoelectrochemical impedance spectroscopy analysis (Fig. 2c), which shows a much smaller circle at the low frequency region under illumination than that in the dark. These observations indicate that the photocurrent was produced by exciting the cell-α-Fe_2O_3 system and governed by the bias.

Coupled electron-hole separation in α-Fe_2O_3 with microbial respiration

The relevance of photocurrent generation to cellular respiration was first explored by measuring the transient photodynamics of electron transfer in the electrochemical system. I~V tests were conducted under intermittent illumination with the α-Fe_2O_3 or cell/α-Fe_2O_3 system. In order to minimize the potential change within each dark-light cycle, a low scan rate of 0.5 mV/s was used in each test. In the absence of *G. sulfurreducens* cells, only a weak anodic photocurrent was generated at above -0.18 V, and the current decayed over time (Fig. 3a). Such a current decay should be ascribed to the capacitive current and temporary trapping of holes at the interface[29]. In contrast, in the presence of active cells on the α-Fe_2O_3 surface, an immediate photocurrent was yielded on illumination in the same voltage range. The photocurrent enlarged until reaching the limiting rate of microbial respiration at potentials above +0.06 V and maintained at 57.2 μA cm^{-2} at even higher potentials. When blocking the electron transfer by selectively inhibiting the electrochemical activity of cyt. c with carbon monoxide, the photocurrent was substantially declined (Supplementary Fig. S4). These results indicate that the electrons for photocurrent production directly came from the respiration of the active cells on the α-Fe_2O_3, and imply that the cells could adjust their respiration to pump out more electrons to the α-Fe_2O_3 under illumination.

The relationship between the light-induced charge separation in the α-Fe_2O_3 and the dissimilatory respiration of *G. sulfurreducens* was examined by analyzing the dynamics of acetate consumption (change of acetate in molar, Δ*acetate*) and the

production of charge under steady cellular respiration conditions. The cells on the electrode surface can pump electrons steadily over time at +0.2 V, accompanied by a proportional consumption of acetate (Supplementary Fig. S5). In the 36-h tests, a positive correlation between the Δ*acetate* and the produced charge was observed, both under illumination and in the dark (Fig. 3b and Supplementary Fig. S6). The fitting curves give the adjusted correlative coefficient R^2 values of 0.9721 and 0.9561, respectively, confirming that the charges were originated from the acetate oxidation by *G. sulfurreducens* cells on the α-Fe_2O_3 surface. In addition, the cells exhibited a similar level of substrate-electricity conversion efficiency regardless the illumination (49.59 % if the consumed acetate was completely oxidized in microbial metabolism). These results indicate that microbial respiration could be driven by the process of light-induced electron transfer at the cell-α-Fe_2O_3 interface, at the same energy efficiency as in dissimilatory respiration in the dark.

Correlation between the light-induced electron transfer and the respiration rate of cells was further examined by monitoring the photocurrent profiles during the biofilm development process at +0.0 V, +0.2 V and +0.6 V, respectively, with periodic illumination. At different biofilm growth stages, the generated photocurrent was plotted to the dark current to characterize the promotion of light-excitation to the microbial respiration rate (Fig. 4a). The anodic photocurrent appeared immediately after the adhesion of *G. sulfurreducens* biofilm onto the α-Fe_2O_3 surface (Fig. 4a and Supplementary Fig. S7). After 100 min of colonization on the α-Fe_2O_3, the cells

produced a respiratory current of 0.5 μA in the dark and a photocurrent of 1.4 μA under illumination. The photocurrent increased to 9.4 μA after 40 h, while the dark current was 24.6 μA. The photocurrent correlated linearly with the dark current at different growth stages of biofilms, regardless of the polarization potentials (Fig. 4b-d). The fitting slopes at these three potentials exhibited an average sensitizing efficiency for microbial respiration (the ratio of the photocurrent to the dark current) of 39.6%. Such a photocurrent dependency on the dark current conclusively couples the light-induced charge separation in the α-Fe_2O_3 with the microbial respiration and electron transfer at the *G. sulfurreducens* cell-α-Fe_2O_3 interface.

Physiological activity of *G. sulfurreducens* cells on the light-excited α-Fe_2O_3

G. sulfurreducens can conserve energy to support microbial growth and their physiological activities from the extracellular electron transfer[30]. However, one main concern of using light-induced electron transfer of semiconductors for respiration is their biotoxicity, as the generation of light-excited holes and radicals may damage the attached cells[18,19] and make the light-induced charge transfer unsustainable. To examine this possibility, the impact of light-exciting α-Fe_2O_3 on the vitality of cells was investigated by measuring the accumulated reducing power in the biofilm under illumination. The global redox state of cyt. c was used as an indicator of accumulated reducing power within healthy cells. The UV-visible spectrum of cyt. c exhibits three characteristic absorption peaks at 419, 522, and 552 nm[31] (Fig. 5a and Supplementary

223 Fig. S8). The results show that the peaks area at 522 and 552 nm had no distinct
224 change before and after the illumination, implying that the cellular activity was not
225 affected by the light-induced holes on the α-Fe_2O_3 surface. To confirm this, the spatial
226 configuration of cellular activities in the biofilm was further examined by measuring
227 the fluorescence counts of the reduced enzymes labeled with a fluorogenic redox
228 sensor. The dye yielded green fluorescence after being reduced by bacterial reductases,
229 which are mostly located as the electron transport complexes in the respiration system.
230 Thus, the fluorescence intensity is proportional to the amount and reductive activity of
231 healthy cells. Consistent with the results on the global redox state, the fluorescence
232 analysis confirms that the biofilm on the α-Fe_2O_3 retained a high activity despite of
233 illumination (Fig. 5b and c). Interestingly, the cells in the middle layers of the biofilm
234 exhibited the highest activity (Fig. 5b and Supplementary Fig. S9), while those near
235 the α-Fe_2O_3 surface had a relatively lower activity, indicating a spatial and functional
236 heterogeneity of the active cells on the α-Fe_2O_3 surface. The weaker fluorescence at
237 the bottom layer of biofilm was possibly attributed to the less availability of acetate
238 and more efficient electron transfer in this region.
239
240 **Discussion**
241
242 The semiconductor-based photoanodes are widely collocated with chemical redox
243 couples such as I^-/I^{3-} in electrolyte for charge transfer at electrode surface in solar

cells[12]. Recently successful photocurrent production with microbial cultures as the electrolyte and α-Fe_2O_3 as the photoanode has been demonstrated[10,14]. To reveal the mechanism of photocurrent production and the involvement of microbial cells in light-driven electron transfer, the direct interplay between *G. sulfurreducens* cells and α-Fe_2O_3 under light-excitation was explored in this work. With the constructed direct physical interface between the cells and α-Fe_2O_3, the light-driven electron transfer across them was accomplished. The experimental results on I_{photo}~V relationship (Fig. 2b and 3a) and CO inhibition clearly show that the photocurrent was entirely originated from the microbial catalysis on the α-Fe_2O_3 surface. In addition, the substrate consumption and respiration activities of cell layer correlated with the photocurrent intensity well, demonstrating the gated dissimilatory respiration of *G. sulfurreducens* driven by the light-induced electron transfer at the α-Fe_2O_3 surface. Such a direct electron transfer process from *G. sulfurreducens* cells to the light-excited α-Fe_2O_3 and is different from that for *S. oneidensis*, which may contribute to the photocurrent production in electrochemical systems by mediating electron transfer to the α-Fe_2O_3 mainly via extracellular flavins[16,17].

Based on the above experimental results and the thermodynamic considerations, we propose a model to describe the electron transfer at the interface between *G. sulfurreducens* cells and light-excited α-Fe_2O_3 (Fig. 6a). In the respiration of *G. sulfurreducens*, electrons produced from acetate oxidation are transferred to the extracellular conductive components, which might be composed by pili[32] and cyt. c

such as OmcZ[33], and then further injected into the Fe(3d) conduction band on the α-Fe_2O_3 surface in the dark. The electron transfer from the reduced cellular components to the Fe(3d) band is slower in kinetics[34], compared to the intracellular catalytic reactions. In the presence of illumination, the photo-excitation of α-Fe_2O_3 brings about much more free electrons to Fe(3d) band by transition, which improves the intrinsic conductivity of α-Fe_2O_3, and leaves holes in the O(2p) valence band. These holes could be drawn from the body of α-Fe_2O_3 by the internal electric field to the cells/α-Fe_2O_3 interface, where they work as the 'active vacancies' (with a high potential of +2.48 V, Supplementary Fig. S3) and open a new electron conduit bridging the redox centers of conductive cellular components to these vacancies at the cell/α-Fe_2O_3 interface. Then, the oxidized cyt. c in the electron transfer chain is regenerated more efficiently to stimulate the cellular respiration (Figs. 3b and 5b). From the results in this work, the ratio of the electrons flowing through the conduction band and valence band is estimated to be 5:2 under illumination (Fig. 6a). Moreover, the injected electrons in α-Fe_2O_3 would be further delivered to the ITO electrode, rather than dissolving Fe(III) to Fe^{2+}.

Previous studies have shown that microbial cells on light-excited semiconductors suffered from metabolic suppression due to an in-situ generation of hydroxyl radicals on semiconductor surface[19,35]. However, this phenomenon was not observed at the cell-α-Fe_2O_3 interface in our system. One possible reason is that the surface holes generated on crystalline iron-oxides are more moderate as compared with other

semiconductors, bringing about a significant thermal barrier to hinder the hole transfer on the α-Fe_2O_3 surface[36,37]. Besides, holes would rapidly combine with the electrons delivered by microbial cells before reacting with the water molecules to form radicals[38]. As a consequence, a high activity could be maintained by the cells on the α-Fe_2O_3 surface as long as the electron output is sustained via the respiration. The light-generated holes on the α-Fe_2O_3 surface are proven to drive cellular respiration at the same energy efficiency to the dark respiration (Fig. 3b). These features gift the essential foundation for microbial dissimilatory respiration on light-excited semiconductors in natural environments and provide an application potential for photo-bioelectrochemical energy technologies.

The respiration driven by the light-induced electron transfer from DMRM to Fe(III) oxides reveals the diversity of microbial energy metabolism in the environment. Although the Fe(III) oxides are present as the predominant iron minerals in most of soils and sediments at circumneutral pH, DMRM respiration on these acceptors is practically hard because of the limited rate of heterogeneous electron transfer from bacterial cells to mineral surface[4]. Redox potentials of crystalline Fe(III)/Fe(II) are hundreds of millivolts negative and supply very little energy to cells through the oxidative phosphorylation[39]. Coupled with the insufficient availability of carbon sources, the DMRM species are often limited in their environmental abundance[40,41]. Our study shows that light-excitation of hematite switches on a new type of electron transfer at the interface with a 40% improvement to the respiration

rate of DMRM, which may greatly favor the microbial growth and proliferation. Therefore, this strategy gives DMRM species an extraordinary competitive advantage over other co-existing bacteria in the ecosystems.

The light-driven electron transfer from *G. sulfurreducens* to hematite may also exert an impact on the speciation of environmental elements. Both dissimilatory respiration and photochemistry of hematite occur in diverse anoxic sites with sufficient light irradiation[8,42,43], and may release Fe^{2+} through injecting electrons into the surface lattices of Fe(III) oxides. The reactive electrons accumulated on α-Fe_2O_3 could also be transferred to other acceptors as long as their reduction potentials are higher than -0.2 V, which are sufficient to drive the light-induced electron transfer when *G. sulfurreducens* cells are respiring on α-Fe_2O_3 surface (Fig. 2b). Thus, it is thermodynamically possible for the *G. sulfurreducens*/α-Fe_2O_3 system to reduce many natural acceptors (e.g., nitrate, humic substances, and oxygen)[44,45], and pollutants (e.g., Cr(VI), nitroaromatic and chlorinated organics)[46-48]. Thus, a light-promoted remote electron transfer from DMRB cells to iron-oxides in natural environments might be associated with the microbial mineralization of organic carbon[49] and reductive transformation of many natural elements (Fig. 6b).

Methods

Growth medium and biofilm formation on electrodes

G. sulfurreducens DL-1 was donated by Prof. Lovley from the University of Massachusetts (USA) and was routinely cultivated in modified DMSZ medium supplemented with 20 mM acetate and 50 mM fumarate. Development of *G. sulfurreducens* biofilm was accomplished in a three-electrode cell with ITO or α-Fe_2O_3/ITO electrode as the working electrode. The mineral solution of culture medium dosed with 20 mM acetate was used as the electrolyte. The electrode potential was set at +0.0 V, +0.2 V, or +0.6 V. All microbial incubation and electrochemical tests were conducted at 30 °C. The details about cell cultivation and biofilm development on the electrodes are given in Supplementary Methods.

Preparation of the α-Fe_2O_3 electrodes

The α-Fe_2O_3 electrodes were prepared through electrophoretic deposition of α-Fe_2O_3 nanoparticles (30 nm) on the ITO electrodes[50]. Briefly, 80 mg α-Fe_2O_3 nanoparticles and 20 mg iodine were dispersed in 100 mL acetone under 30-min sonication. The mixture was stirred before electrodeposition. An external bias of -10 V was applied between two parallel ITO electrodes and kept for 2 min. The as-prepared electrodes were calcined at 673 K for 30 min. For the UV-visible spectroscopy tests, the α-Fe_2O_3 nanoparticles were electrodeposited for 30 s on ITO to improve its light transmittance.

Electrochemical and photoelectrochemical measurements

The amperometric i-t curves and cyclic voltammetry analysis during biofilm development on the electrodes were performed with a multi-potentiostat (CHI 1030A, CH Instruments Inc., China). During biofilm development, a blended fluorescent mercury lamp (250W, Yaming Lighting Co., China) was used as the light source for photocurrent tests. The lamp and electrochemical cells were placed in an incubator at 30 °C.

The open-circuit potential, current-potential curves, and photoelectrochemical impedance spectroscopy (PEIS) of the mature biofilm on the α-Fe_2O_3 electrode were recorded using an electrochemical working station (CHI 660C, CH Instruments Inc., China). A xenon lamp fitted with a cutoff filter to irradiate visible light (λ> 400 nm) was used as the light source. The power of xenon lamp was 400 W for the open-circuit potential and current-potential curves tests and 200 W for the PEIS analysis.

Vitality of biofilm

For confocal laser scanning microscopy (CLSM) imaging, the illuminated and unilluminated samples were transferred into an anaerobic glove box and immediately incubated in 50 mM phosphate buffer containing 1 ‰ RedoxSensor™ Green reagent A (Invitrogen Co., USA) at 30 °C in the dark. After 1 h, the samples were gently rinsed with phosphate buffer to remove the unbound residual dye from the biofilm matrix. Then, the samples were covered with antifade solution and imaged with a

fluorescent microscope (FV1000, OLYMPUS Co., Japan). Z-series images were processed and analyzed with FV10-ASW at an excitation wavelength of 490 nm.

To measure the acetate consumption, the biofilm was developed on the α-Fe_2O_3 surface at +0.2 V. Then, the electrolyte was replaced with fresh medium containing 2 mM acetate. In order for the comparability of bioactivity between electrochemical cells, only the biofilms exhibited approximate dark currents were used in this experiment. The α-Fe_2O_3 layer was illuminated with the blended fluorescent mercury lamp at +0.2 V. Intermittent illuminations (dark/light, 15 min/15 min) were applied in order to prevent photochemical deterioration of the α-Fe_2O_3 layer. The acetate concentration in electrolyte was measured every 6 h. Amperometric i-t curves were integrated to calculate the coulombs of electric charge.

Scanning electron microscopy

Samples for environmental scanning electron microscopy (ESEM) were withdrawn from the electrochemical cells and crosslinked with 2.5% glutaraldehyde for 7 days at 4 °C. The samples were examined with a FEI ESEM (FEI Co., USA) at 20 kV under wet mode. The stage temperature was 280 K with a chamber pressure of 800 Pa to maintain a relative humidity of 80% for the sample. Samples for scanning electron microscopy (SEM) were crosslinked with 2.5% glutaraldehyde for 12 h at 4 °C. Then, the samples were serially dehydrated with ethanol of 30%, 50%, 70%,

80%, 95%, and 100%, each for 30 min. Finally, the samples were dried with hexamethyl disilylamine.

Conclusions

In this study, we provide evidences about the visible light-excited direct electron transfer from *G. sulfurreducens* cells to naturally-abundant Fe(III) oxide, α-Fe_2O_3, for microbial respiration and examine the physiological activity of *G. sulfurreducens* in this process. Our results suggest that light-driven, direct electronic communication between DMRM cells and the inorganic minerals is ubiquitous in the natural environment. Such an electron transfer provides a unique way of energy metabolism for DMRM species in nature, which expands our understanding about the diversity of microbial respiration and may have an important impact on the compositions and abundance of microbial populations, where dissimilatory iron reduction is feasible. In addition, the direct electron transfer from microorganisms to light-excited semiconductors suggests a great potential of utilizing photoanodes and non-phototrophic DMRM species for bioelectrochemical applications.

Acknowledgements

This work is partially supported by the Program for Changjiang Scholars and Innovative Research Team in University, China. We thank Prof. D. R. Lovley from

the University of Massachusetts for providing the bacterial strain used in this work. Also, we thank Mr. Liuer Wu and Dr. Shijing Tan for helpful discussion.

Notes and references

1 D. R. Lovley, *Energy Environ. Sci.*, 2011, 4, 4896-4906.

2 D. R. Lovley and K. P. Nevin, *Curr. Opin. Biotechnol.*, 2011, 22, 441-448.

3 X.-W. Liu, W.-W. Li and H.-Q. Yu, *Chemical Society Reviews*, 2014, DOI: 10.1039/C1033CS60130G.

4 D. R. Lovley, D. E. Holmes and K. P. Nevin, in *Advances in Microbial Physiology*, ed. R. K. Poole, Academic Press Ltd-Elsevier Science Ltd, London, 2004, 49, pp. 219-286.

5 L. A. Shi, D. J. Richardson, Z. M. Wang, S. N. Kerisit, K. M. Rosso, J. M. Zachara and J. K. Fredrickson, *Environ. Microbiol. Rep.*, 2009, 1, 220-227.

6 D. J. Richardson, J. N. Butt, J. K. Fredrickson, J. M. Zachara, L. Shi, M. J. Edwards, G. White, N. Baiden, A. J. Gates, S. J. Marritt and T. A. Clarke, *Mol. Microbiol.*, 2012, 85, 201-212.

7 R. M. Cornell and U. Schwertmann, *The Iron Oxides: structure, Properties, Reactions, Occurrences and Uses*, Wiley-VCH, 2003.

8 K. A. Weber, L. A. Achenbach and J. D. Coates, *Nat. Rev. Microbiol.*, 2006, 4, 752-764.

9 B. H. Lower, L. Shi, R. Yongsunthon, T. C. Droubay, D. E. McCready and S. K. Lower, *J. Bacteriol.*, 2007, 189, 4944-4952.

10 R. Nakamura, F. Kai, A. Okamoto, G. J. Newton and K. Hashimoto, *Angew. Chem.-Int. Edit.*, 2009, 48, 508-511.

11 B. Klahr, S. Gimenez, F. Fabregat-Santiago, J. Bisquert and T. W. Hamann, *Energy Environ. Sci.*, 2012, 5, 7626-7636.

12 M. Gratzel, *Nature*, 2001, 414, 338-344.

13 R. Nakamura, F. Kai, A. Okamoto and K. Hashimoto, *J. Mater. Chem. A*, 2013, 1, 5148-5157.

14 F. Qian, H. Wang, Y. Ling, G. Wang, M. P. Thelen and Y. Li, *Nano Lett.*, 2014, 14, 3688-3693.

15 K. Kamada, A. Moriyasu and N. Soh, *J. Phys. Chem. C*, 2012, 116, 20694-20699.

16 X. C. Jiang, J. S. Hu, L. A. Fitzgerald, J. C. Biffinger, P. Xie, B. R. Ringeisen and C. M. Lieber, *Proc. Natl. Acad. Sci. U. S. A.*, 2010, 107, 16806-16810.

17 N. J. Kotloski and J. A. Gralnick, *mBio*, 2013, 4.

18 P. Basnet, G. K. Larsen, R. P. Jadeja, Y. C. Hung and Y. P. Zhao, *ACS Appl. Mater. Interfaces*, 2013, 5, 2085-2095.

19 P. C. Maness, S. Smolinski, D. M. Blake, Z. Huang, E. J. Wolfrum and W. A. Jacoby, *Appl. Environ. Microbiol.*, 1999, 65, 4094-4098.

20 D. R. Lovley, T. Ueki, T. Zhang, N. S. Malvankar, P. M. Shrestha, K. A. Flanagan, M. Aklujkar, J. E. Butler, L. Giloteaux, A. E. Rotaru, D. E. Holmes, A. E. Franks, R. Orellana, C. Risso and K. P. Nevin, in *Advances in Microbial Physiology, Vol 59*, ed. R. K. Poole, Academic Press Ltd-Elsevier Science Ltd, London, 2011, 59, pp. 1-100.

21 D. R. Bond and D. R. Lovley, *Appl. Environ. Microbiol.*, 2003, 69, 1548-1555.

22 A. J. Frierdich and J. G. Catalano, *Geochim. Cosmochim. Acta*, 2012, 91, 240-253.

23 R. M. Snider, S. M. Strycharz-Glaven, S. D. Tsoi, J. S. Erickson and L. M. Tender, *Proc. Natl. Acad. Sci. U. S. A.*, 2012, 109, 15467-15472.

24 D. R. Bond, S. M. Strycharz-Glaven, L. M. Tender and C. I. Torres, *ChemSusChem*, 2012, 5, 1099-1105.

25 H. Richter, K. P. Nevin, H. F. Jia, D. A. Lowy, D. R. Lovley and L. M. Tender, *Energy Environ. Sci.*, 2009, 2, 506-516.

26 Y. Liu, H. Kim, R. R. Franklin and D. R. Bond, *ChemPhysChem*, 2011, 12, 2235-2241.

27 K. Fricke, F. Harnisch and U. Schroder, *Energy Environ. Sci.*, 2008, 1, 144-147.

28 D. M. Sherman, *Geochim. Cosmochim. Acta*, 2005, 69, 3249-3255.

29 L. M. Peter, in *Comprehensive Chemical Kinetics*, eds. R. G. Compton and G. Hancock, Elsevier, 1999, 37, pp. 223-280.

30 K. P. Nevin, H. Richter, S. F. Covalla, J. P. Johnson, T. L. Woodard, A. L. Orloff, H. Jia, M. Zhang and D. R. Lovley, *Environ. Microbiol.*, 2008, 10, 2505-2514.

31 Y. Liu and D. R. Bond, *ChemSusChem*, 2012, 5, 1047-1053.

32 S. M. Strycharz-Glaven, R. M. Snider, A. Guiseppi-Elie and L. M. Tender, *Energy Environ. Sci.*, 2011, 4, 4366-4379.

33 K. Inoue, C. Leang, A. E. Franks, T. L. Woodard, K. P. Nevin and D. R. Lovley, *Environ. Microbiol. Rep.*, 2011, 3, 211-217.

34 K. Sivula, F. Le Formal and M. Gratzel, *ChemSusChem*, 2011, 4, 432-449.

35 E. Dumas, C. Gao, D. Suffern, S. E. Bradforth, N. M. Dimitrijevic and J. L. Nadeau, *Environ. Sci. Technol.*, 2010, 44, 1464-1470.

36 Y. Xu and M. A. A. Schoonen, *Am. Miner.*, 2000, 85, 543-556.

37 A. J. Cowan, C. J. Barnett, S. R. Pendlebury, M. Barroso, K. Sivula, M. Gratzel, J. R. Durrant and D. R. Klug, *J. Am. Chem. Soc.*, 2011, 133, 10134-10140.

38 G. F. White, Z. Shi, L. Shi, Z. M. Wang, A. C. Dohnalkova, M. J. Marshall, J. K. Fredrickson, J. M. Zachara, J. N. Butt, D. J. Richardson and T. A. Clarke, *Proc. Natl. Acad. Sci. U. S. A.*, 2013, 110, 6346-6351.

39 B. Thamdrup, in *Advances in microbial ecology*, Kluwer Academic/Plenum Publishers, New York, 2000, 16, pp. 41-84.

40 D. E. Holmes, K. T. Finneran, R. A. O'Neil and D. R. Lovley, *Appl. Environ. Microbiol.*, 2002, 68, 2300-2306.

41 D. Sarkar, M. Ferguson, R. Datta and S. Birnbaum, *Environ. Pollut.*, 2005, 136, 187-195.

42 D. A. S. Finden, E. Tipping, G. H. M. Jaworski and C. S. Reynolds, *Nature*, 1984, 309, 783-784.

43 K. L. Straub, M. Benz and B. Schink, *FEMS Microbiol. Ecol.*, 2001, 34, 181-186.

44 L. J. Bird, V. Bonnefoy and D. K. Newman, *Trends Microbiol.*, 2011, 19, 330-340.

45 C. Siffert and B. Sulzberger, *Langmuir*, 1991, 7, 1627-1634.

46 R. Nakamura, K. Kamiya and K. Hashimoto, *Chem. Phys. Lett.*, 2010, 498, 307-311.

47 H. Mekatel, S. Amokrane, B. Bellal, M. Trari and D. Nibou, *Chem. Eng. J.*, 2012, 200, 611-618.

48 J. Braunschweig, J. Bosch and R. U. Meckenstock, *New Biotech.*, 2013, 30, 793-802.

49 A. H. Lu, Y. Li, X. Wang, H. R. Ding, C. P. Zeng, X. X. Yang, R. X. Hao, C. Q. Wang and M. Santosh, *Precambrian Res.*, 2013, 231, 401-408.

50 K. Maeda, M. Higashi, B. Siritanaratkul, R. Abe and K. Domen, *J. Am. Chem. Soc.*, 2011, 133, 12334-12337.

Figure legends

Fig. 1 Electrochemical interface between *G. sulfurreducens* cells and α-Fe_2O_3. (a) Schematic diagram of the experimental architecture (not to scale) of the interface in our work. The electrochemical layers consisted of *G. sulfurreducens* cells, α-Fe_2O_3, and conductive ITO substrate. The arrow refers to the direction of electron flow; (b) Dynamics of anodic current during the cell layers development at poised potential +0.200 V vs. SHE; (c) The cross section of the α-Fe_2O_3/ITO electrode covered with layers of cell. Upward from the bottom: ITO glass, α-Fe_2O_3, and biofilm at the edge of electrode; (d) Mature cell layers on the α-Fe_2O_3 surface; (e) Cyclic voltammetry of active cells on an ITO electrode with acetate in the electrolyte. Different scan rates were applied to distinguish the polarized potentials-dependent catalytic currents and the reversible oxidation and reduction of cyt. c close to the ITO surface; and (f) Potentials transient decay after the cell/α-Fe_2O_3 was disconnected from the potentiostat. The tests were conducted twice and the results are identical.

Fig. 2 Photoelectrochemical characterization of the cell/α-Fe_2O_3 system. The mature cell layers developed on the α-Fe_2O_3 electrodes at +0.2 V were used for the tests. (a) Current profiles on illuminating the cell/α-Fe_2O_3 at +0.2 V. Repeated tests with three cell/α-Fe_2O_3 electrodes are shown; (b) I~V curves of the cell/α-Fe_2O_3 electrode under illumination and in the dark. Voltammetric tests were conducted from +0.6 V to -0.45 V at scanning rate of 0.5 mV/s. According to the redox potentials, charge transfer at the cells/α-Fe_2O_3 interface is suppressed (*Region I*), limited by the potential (*Region II*), or limited by cellular respiration (*Region III*). The differences between currents (i.e. photocurrents) vs. potentials were shown with violet dots; and (c) Photoelectrochemical impedance spectroscopy of the cell/α-Fe_2O_3 electrode under illumination and in the dark at +0.2 V. The frequency was changed from 100 kHz to 0.01 Hz with an amplitude of 10 mV. Chronoamperometry at +0.2 V was conducted before each test until reaching the steady state. This experiment was conducted with six replicates and the representative results are shown.

Fig. 3 The role of microbial catalysis in photocurrent production. (a) Current-potential curves of the biofilm/α-Fe_2O_3 electrode and α-Fe_2O_3 electrode under intermittent illumination. Voltammetry was conducted by varying the potential from -0.48 V to +0.66 V at 0.5 mV/s. The dotted line shows the dark current for the biofilm/α-Fe_2O_3 electrode. A xenon lamp, fitted with a cutoff filter to irradiate visible light ($\lambda > 400$ nm), was used as the light source. (b) Linear correlation between the acetate consumption during microbial respiration and the charge quantity passing through the cells-α-Fe_2O_3 interface. Intermittent illumination was applied in order to prevent possible photochemical deterioration of the α-Fe_2O_3 layer under long-time illumination as shown in Supplementary Fig. S6. Error bars indicate the standard error of the duplicate tests.

Fig. 4 Dependence of photocurrent on the respiration rate of *G. sulfurreducens* cells on α-Fe_2O_3 surface. (a) The photocurrent evolution profiles during biofilm development on the α-Fe_2O_3 surface at +0.200 V. Intermittent illumination was provided at 10-min irradiation and 80-min interval. A fluorescent mercury lamp was used as light source; B-D, Linear correlation of steady-state photocurrent to dark current contributed by the microbial respiration at (b) +0.000 V, n=152; (c) +0.200 V, n=122; and (d) +0.600 V, n=112. The values of dark current were collected before each illumination. 95% confidence bands are shown for each fitting.

Fig. 5 Physiological activity of *G. sulfurreducens* cells on the α-Fe_2O_3 surface under illumination. (a) UV-Vis absorbance of *G. sulfurreducens* biofilm on the α-Fe_2O_3 surface before and after illumination for 20 min. The cell/α-Fe_2O_3 system was kept in open circuit for 100 s to get fully reduced cells before each test. UV-Vis absorbance of the α-Fe_2O_3 layer and ITO had been deducted from the results; (b) Spatial configuration of cellular activities in the biofilms. The cells on the α-Fe_2O_3 surface were stained with RedoxSensor dye and the fluorescence intensity represented the (respiratory) reductases activity. The normalized fluorescence intensity at each sampling plane (parallel to the surface) was plotted to the distance from the α-Fe_2O_3 layer (Z = 0); (c) Typical 3D pattern of fluorescence intensity of cell layers on the illuminated α-Fe_2O_3 surface. The tests were repeated four times and the representative data are shown.

Fig. 6 Schematic diagrame of charge transfer at the interface between cells andα-Fe_2O_3 under illumination. (a) Schematic diagram of charge transfer in the experimental set-up. Light with wavelengths below 563.4 nm is needed to effectively promote electrons into the Fe(3d) conduction band and leave holes in the O(2p) band. The *G. sulfurreducens* cells supply electrons to the both the holes on α-Fe_2O_3 surface and the Fe(3d) conduction band during acetate metabolism. The accumulated electrons in the conduction band were collected with an electrode. (b) mechanism of light-driven charge transfer in the environment with possible natural electron acceptors to collect electrons in the conduction band of α-Fe_2O_3.

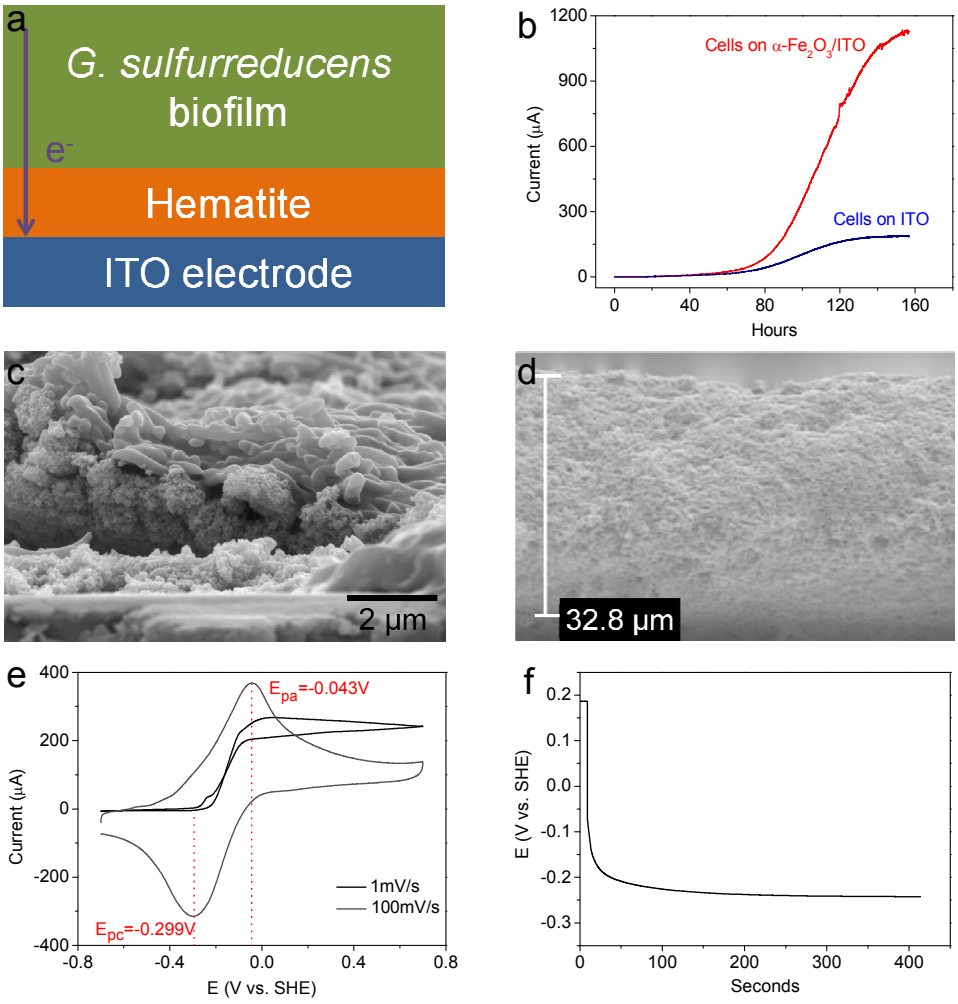

Figure 1

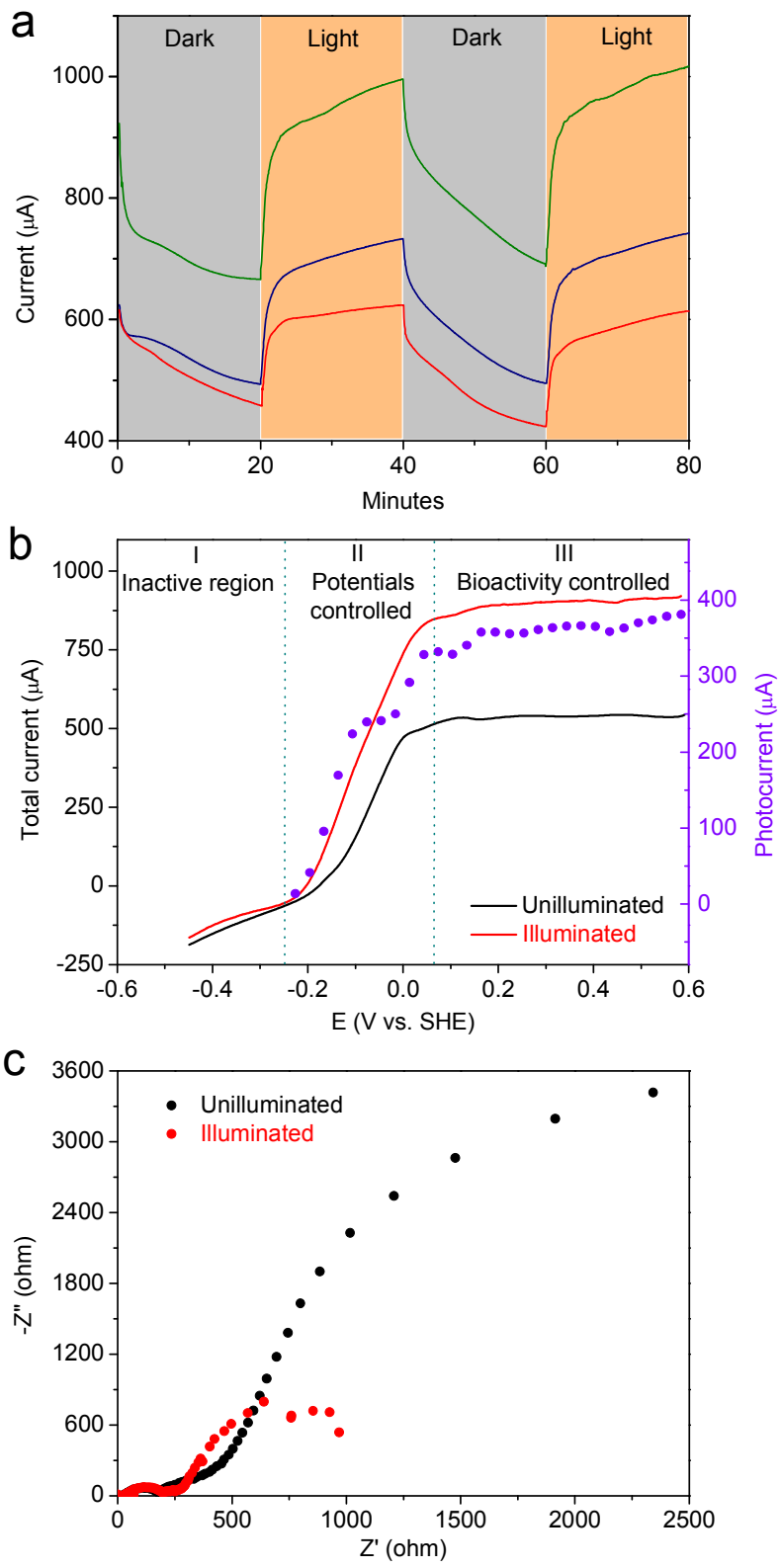

Figure 2

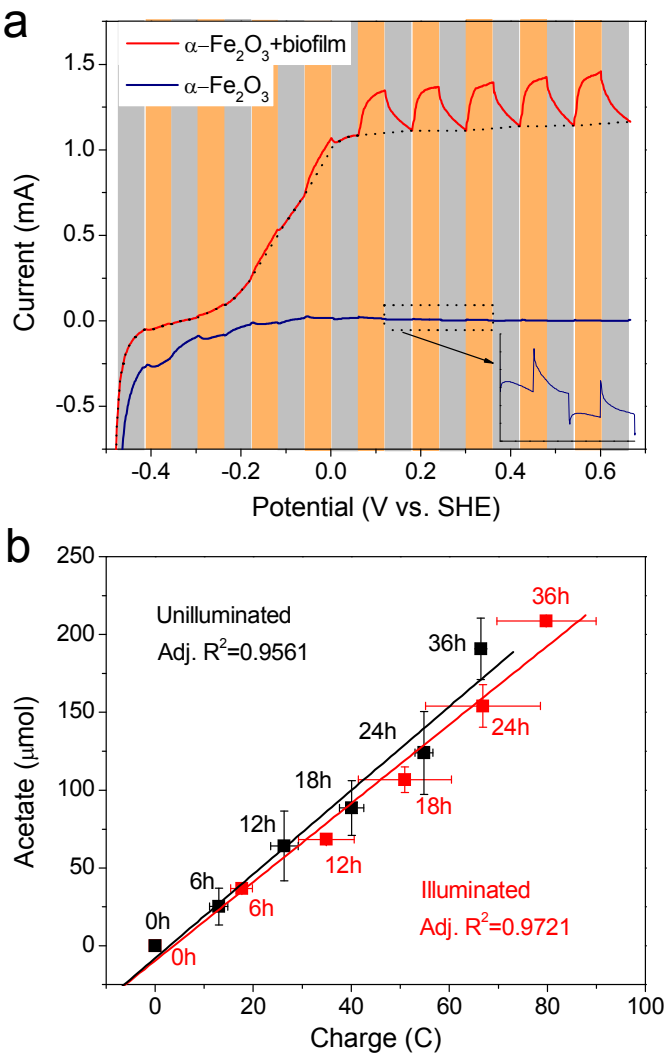

Figure 3

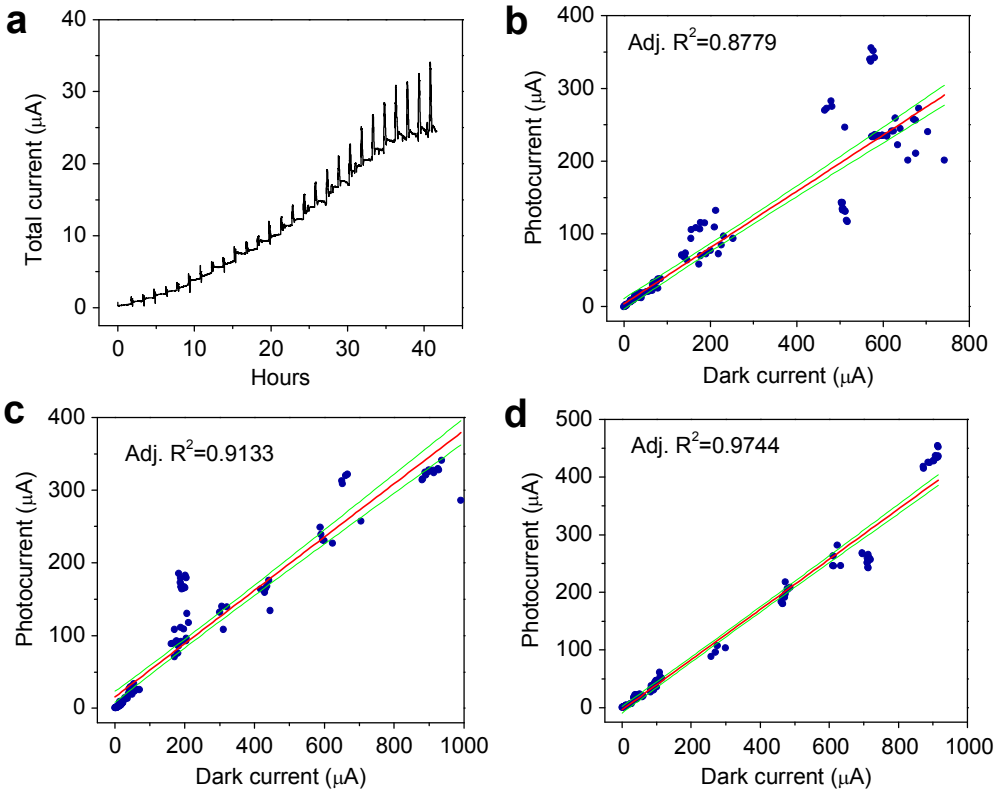

Figure 4

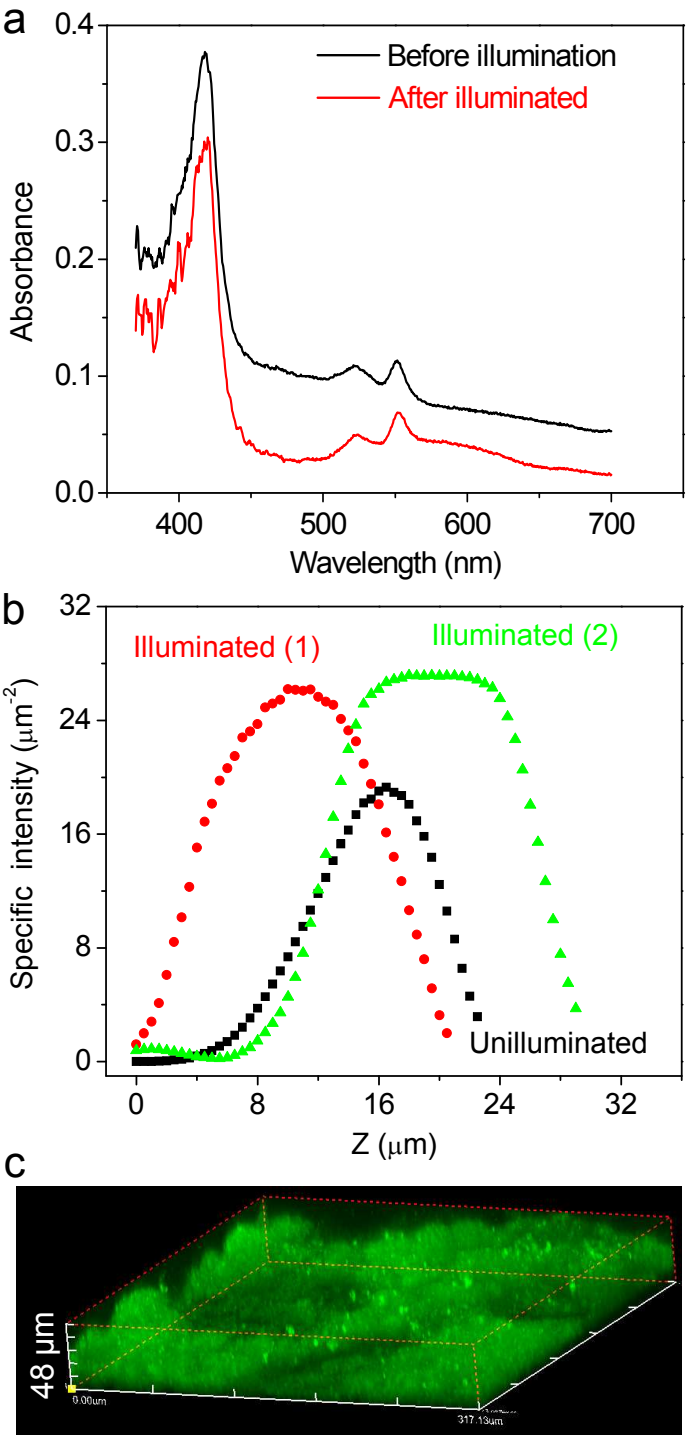

Figure 5

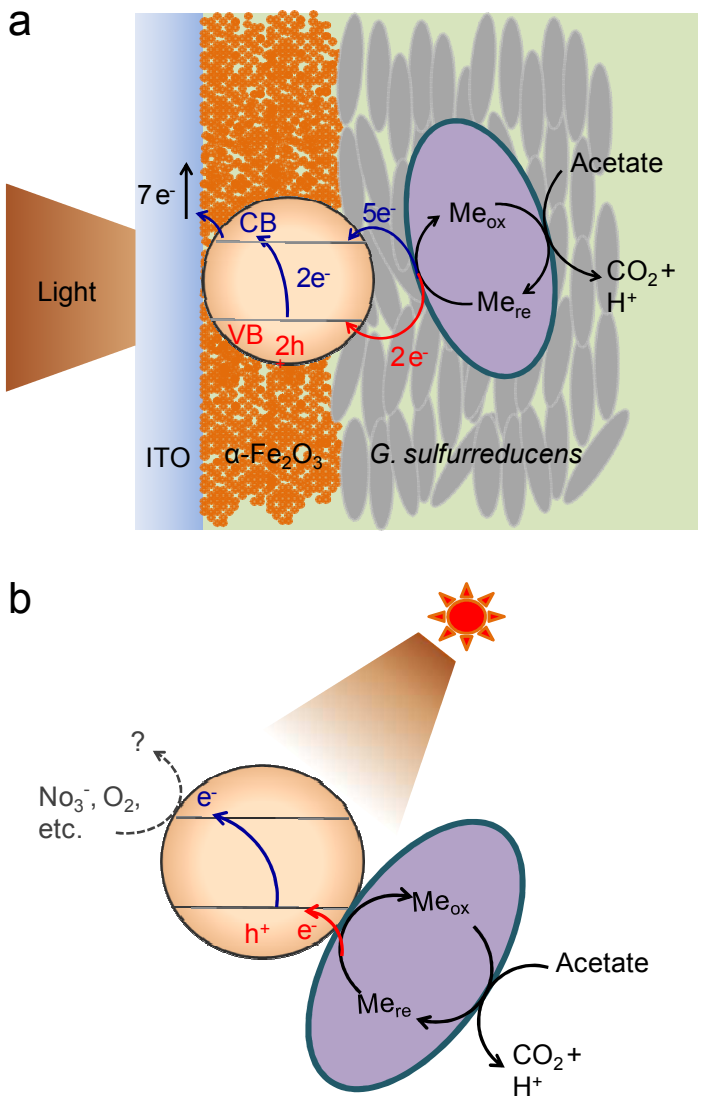

Figure 6